Some New Results of Quantum Simulator NEMO-VN2

Dinh Sy Hien

Department of Electronics, HCM University of Science
227 Nguyen Van Cu Street, District 5, HoChiMinh City, Vietnam
dshien52@yahoo.com

Abstract- **We have developed NEMO-VN2, a quantum device modeling tool that simulates quantum devices including the resonant tunneling diode, the single electron transistor, the molecular field effect transistor, the carbon nanotube field effect transistor. In the simulator the non-equilibrium Green's function is used to perform a comprehensive study of emerging nanoelectronics devices. The program has been written by using graphic user interface of Matlab. NEMO-VN2 uses Matlab to solve Schrodinger equation with Poisson equation to get current-voltage characteristics of quantum devices. In the report, we describe the upgraded simulator, provide a short overview of the theoretical methodology using non-equilibrium Green's function for modeling of nanoscale devices and typical simulations related to spin field effect transistor and graphene field effect transistor used to illustrate the capabilities of the NEMO-VN2.**

Keywords- Spin Transistor; Spin Field Effect Transistor; Graphene; Graphene Field Effect Transistor; Current-Voltage Characteristics.

I. INTRODUCTION

The dimentional scaling of CMOS device and process technology will become much more difficult as the semiconductor industry approaches 10 nm (6 nm physical channel length) around year 2019 and will eventually approach asymptotic end according to the International Technology Roadmap for Semiconductor for emerging research devices [1]. Beyond this period of traditional CMOS it may be possible to continue functional scaling by integrating alternative electronic device on to a silicon platform. These alternative electronic devices include 1D structures such as carbon nanotube field effect transistor (CNTFET), resonant tunneling diode (RTD), single electron transistor (SET), molecular field effect transistor (MFET), spin field effect transistor (SPINFET), and graphene field effect transistor (GFET).

We have developed NEMO-VN2 [2, 3, 4], a quantum device modeling tool that simulates a wide variety of quantum devices including the resonant tunneling diode, the single electron transistor, the molecular field effect transistor, the carbon nanotube field effect transistor, since its inception in 2010. In the simulator, the non-equilibrium Green's function is used to perform a comprehensive study of emerging nanoelectronics devices. The program has been written by using graphic user interface of Matlab. NEMO-VN2 uses Matlab to solve Schrodinger equation with the Poisson equation to get current-voltage characteristics of quantum devices.

In recent years, a vigorous research effort to demonstrate spin transistors has been pursued. One of the motivations has been that spin transistors are identified as one of the most promising alternatives to traditional MOSFET by the International Technology Roadmap for Semiconductors [1]. Simulations have predicted that spin transistors can scale in their size with smaller switching energy and less overall power dissipation than MOSFET.

The idea of spin field-effect transistor sparked after Fert et al. [5] and Grunberg et al. [6] discovered the giant magneto resistance effect in magnetic multilayer systems in 1988. They found huge differences in current coming out of a magnetic and metallic multilayer system when the magnetic layers had the same or different scattering of electrons. Shortly thereafter room temperature magnetic field sensors were made [7] using spin property which had much better performance than previously used anisotropic magneto-resistance property.

Following the preliminary realization of the potential benefits of utilizing spin property, Datta and Das proposed an electron wave analog of the electro-optic light modulator in the late 1989 [8]. Most of the today's interest in this newly born field of study is motivated by their well-known proposed device which is now known as *spin field-effect transistor* (spin FET).

Graphene [9-16] has been one of the most rigorously studied research materials since its inception in 2004. There has been a lot of study focused on transport properties of graphene [17-20]. Many issues related to transport properties of graphene field-effect transistors (FETs). Experimental [21-24] and theoretical [25-29] studies have shown that even though being a gapless semi-metallic material, a graphene FET shows saturating current-voltage behaviors.

In previous studies [25-29], to describe semi-classical transport of graphene FET at a channel length that a semi-classical Boltzmann transport equation (BTE) is solved self consistently with Poisson equation. Monte-Carlo method and numerical solutions of solving BTE have been implemented, they are limited to two-dimensional k-space, which assumes a homogeneous material and therefore it has limitations to describe transport properties in the graphene transistor accurately.

In this work, to describe transport behaviors of graphene FET at channel length that quantum mechanical Schrodinger wave equation is solved self consistenly with Poisson equation. The non-equilibrium Green's function (NEGF) method [30], which is commonly used for nanoscale devices, has been implemented by using graphic user interface (GUI) of Matlab as discussed in detail later.

This paper reviews the capabilities of the upgraded NEMO-VN2, summarizes the theoretical approach and gives examples of several simulations of the simulator.

II. SIMULATION METHOD AND RESULTS

A. *Non-equilibrium Green's Function Method in Modeling of Quantum*

The NEGF model of the CNTFET used for transport simulations is shown in Fig. 1.

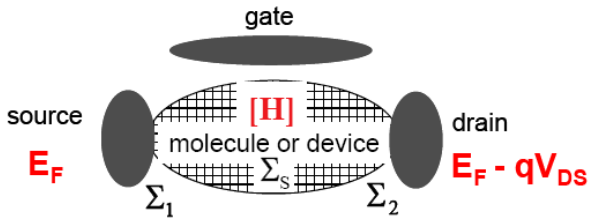

Fig. 1 A generic transistor consists of a device channel connected to source and drain contacts. The source-drain current is modulated by a third electrode, the gate. The quantities involved in NEGF formalism are also shown.

Here, H is the device Hamiltonian, and the self-energy functions $\Sigma_{1,2}$ present the semi-infinite ideal source-drain contacts. Σ_S is the self-energy for the e-ph interaction, and one sets $\Sigma_S = 0$ for the ballistic approximation.

The retarded Green's function for the device in matrix form is given by

$$G(E) = [(E + i\eta^+)I - H - \Sigma(E)]^{-1} \tag{1}$$

where η^+ is an infinitesimal positive value, and I is the identity matrix.

The self-energy contains contributions from all mechanisms of relaxation, which are the source and drain electrodes, and from scattering

$$\Sigma(E) = \Sigma_1(E) + \Sigma_2(E) + \Sigma_S(E) \tag{2}$$

Note that, in (2), the self-energy functions are, in general, energy dependent. The current flows from source to drain can be defined

$$I = \frac{4e}{\hbar}\int_{-\infty}^{+\infty}\frac{dE}{2\pi}T(E)\left[f\left(E - E_S^F\right) - f\left(E - E_D^F\right)\right] \tag{3}$$

where f(E) is the Fermi distribution, and $E_{S/D}^F$ denotes the source and drain Fermi energies, respectively. With the transmission coefficient T(E) given by

$$T(E) = \text{Trace}\,[\Gamma_S(E)G(E)\,\Gamma_D G^+(E)] \tag{4}$$

where level broadening can be defined as follows:

$$\Gamma(E) = i[\Sigma(E) - \Sigma^+(E)] \tag{5}$$

where $\Sigma^+(E)$ represents the Hermitian conjugate of Σ matrix defined by (2).

B. *Some Simulation Results and Discussion*

NEMO-VN2 has a rich variety of simulation models, while this provides the maximum flexibility in term of applicability to types of different devices and test conditions. The problem is that NEMO-VN2 requires over 100 simulation parameters. Traditional device simulators force the users to familiarize themselves with all available simulation parameters and ensure that they are set correctly. To minimize this burden for the users, NEMO-VN2 uses a hierarchical approach to input and display simulation parameter values. The top level of this hierarchy specifies the highest level option (nanodevices). Subsequent levels contain more detailed options such as current-voltage characteristics of devices, types of material, size of devices, temperature, colors, etc.

The main screen shown in Fig. 2a is the central location where the user controls the upgraded NEMO-VN2 simulation. From main screen, the user can choose various types of quantum device simulations by clicking the left mouse pointer on sub-menu of nanodevices (in the left top corner). In this manner, the user can quickly enter the device list and hot keys with minimum of typing. Clicking the left mouse pointer on each item in the device list or using hot keys initiates the selection of models which is used to calculate the current - voltage characteristics (Fig. 2b).

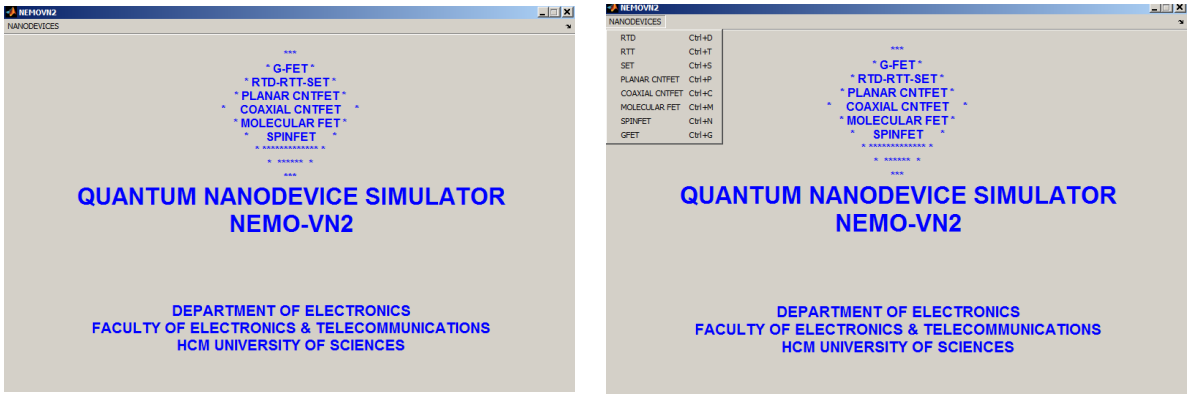

(a) (b)

Fig. 2 a) The upgraded NEMO-VN2 main screen, b) Pressing the left mouse pointer on "NANODEVICES" displays a list of simulation quantum devices.

1) Resonant Tunneling Devices:

The RTDs are two terminal devices that have a very high switching speed and exhibit a region of negative differential resistance in their I-V curves. These two characteristics make them potentially attractive as high-speed switching devices.

Current-voltage characteristics of the RTD are shown in Fig. 3. Characteristic curve is divided into two parts: positive and negative resistances. Here, it should be emphasized that the current peak and the valley currents of the RTD are perfectly represented by the model.

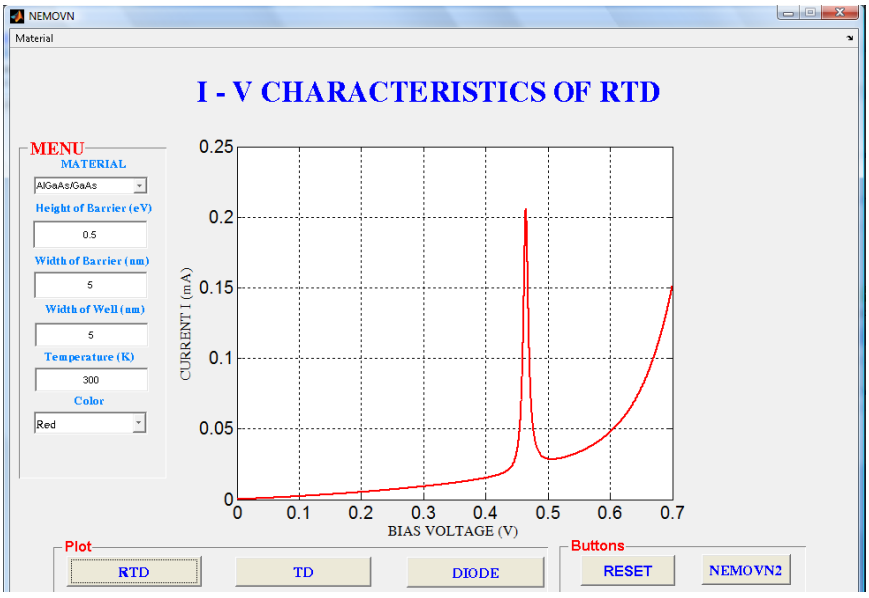

Fig. 3 Current-voltage characteristic of RTD at room temperature

2) Single Electron Transistor:

Single electron transistor is three-terminals device containing source, drain and gate. A model of single electron transistor usually called a capacitance model is shown in Fig. 4. A single electron transistor is made from two tunnel junctions that share a common electrode. A tunnel junction consists of two pieces of metal supported by a very thin (about 1 nm) insulator. The only way for electrons is from one of the metal electrodes to travel to the other electrode is to tunnel through the insulator. Since tunneling is a discrete process, the electric charge that flows through the tunnel junction in multiples of e, the charge of electron.

A quantum dot (QD) is usually formed in two dimensional electron gas (2DEG) in GaAs/AlGaAs using standard electron beam lithography. The quantum dot is connected to the source and drain electrodes through tunnel barriers. The potential in the

dot can be controlled by the gate electrode which is capacitively coupled to the quantum dot (Fig. 4b). The current through the quantum dot can be periodically modulated by the gate voltage. When the current is zero (Coulomb blockade, CB), the number of electrons is fixed. Therefore it differs exactly by one on both sides of the current peak.

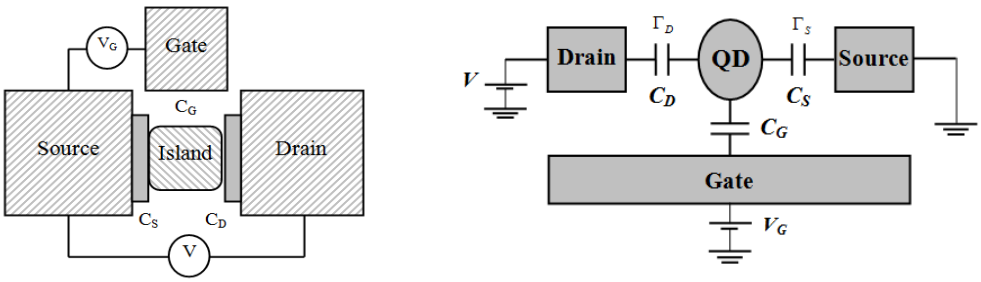

(a) (b)

Fig. 4 a) Structure of single electron transistor, b) equivalent schematic of single electron transistor.The quantum dot is connected to the source and drain electrodes through small tunnel barriers. The potential in the quantum dot can be modified by the gate electrode which is capacitively coupled to the quantum dot, $V_G = (2n+1)e/2C_G$. The DC bias (V_D) is applied and the current is measured as a function of V_D and V_G. The SET's parameters are: C_S, C_D, C_G, Γ_S, Γ_D.

By utilizing the simulator namely NEMO-VN2, the I_D–V_G characteristics of the SET having the given parameters are shown in Fig. 5.

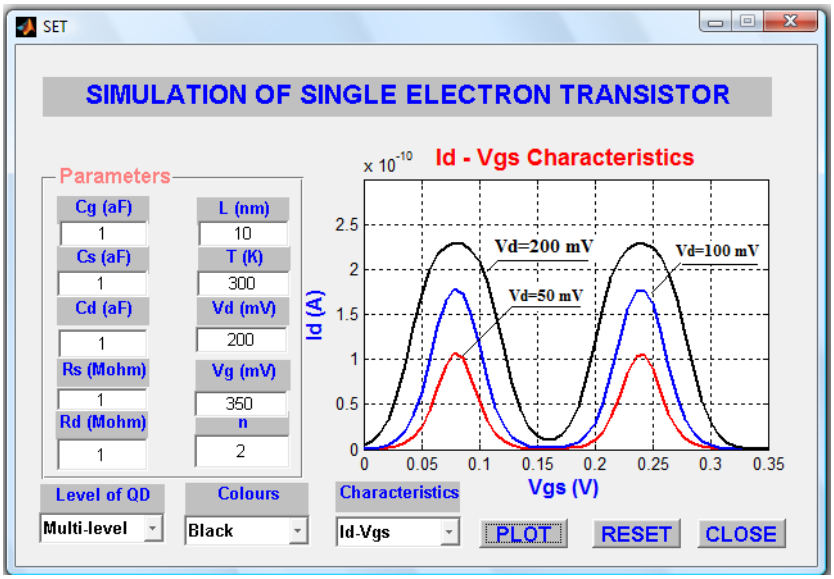

Fig. 5 Typical I_D-V_G characteristics (Coulomb oscillations) of the SET simulated by the simulator NEMO-VN2 for various values of V_D = 50 mV, 100 mV, and 200 mV at room temperature, T = 300 K. The SET device parameters are: L = 10 nm, $C_G = C_S = C_D$ = 1 aF and $R_S = R_D$ = 1 MΩ.

3) Molecular Field Effect Transistor:

Molecular field effect transistor is a promising alternative candidate of traditional MOSFET in future due to its small size, low power and high speed. The structure of the MFET is in shape like traditional MOSFET, but its conductive channel is replaced by a molecule.

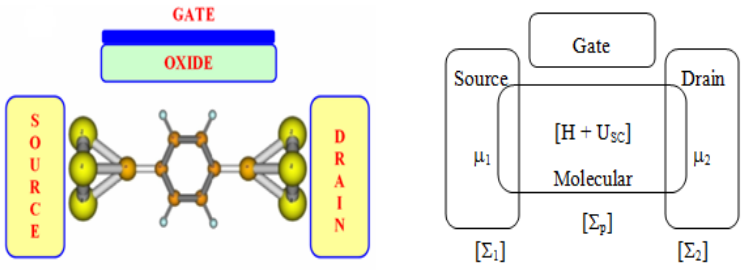

(a) (b)

Fig. 6 (a) Schematic view of a molecule coupled to source and drain contacts, (b) The molecule is described by a Hamiltonian H and a self– consistent potential U_{SC}.The effect of the large contacts is described using self – energy matrices $\Sigma_{1,2}$. Scattering processes may be described using another self – energy matrix Σ_p. The source and drain contacts are identified by their respective Fermi levels μ_1 and μ_2.

Molecular field effect transistor is three terminals device cotaining source, drain and gate. A schematic view of a molecule coupled to gold source (S) and drain (D) contacts is shown in Figure 6. As an example we use the benzene-1,4-dithiol molecule which consists of a phenyl ring with thiol(-SH) end groups. A gate terminal may be used to modulate the conductance of the molecule. The coupling between the gate and the molecule is purely capacitive – there is no gate current.

Current–voltage characteristics of the molecular field effect transistor at different values of bias voltage are shown in Fig. 7.

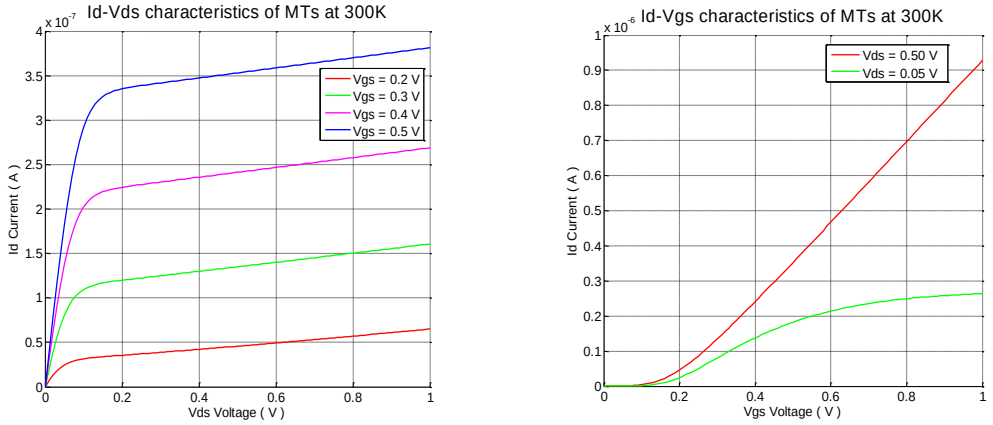

(a) (b)

Fig. 7 Current – voltage characteristics of the MFET: (a) $I_D = f(V_D)$ for different values of the gate voltages and (b) $I_D = f(V_G)$ for different values of the drain voltages.

4) Carbon Nano Tube Field Effect Transistor [2, 3]:

CNTFET is a three-terminals device consisting of a semiconducting nanotube bringing two contacts (source and drain), and acting as a carrier channel, which is turned on or off electrically via the third contact (gate). Presently, there are several types of CNTFETs have been fabricated, but CNTFET geometries may be grouped in two major categories: planar and coaxial CNTFETs, whether planar or coaxial, relies on simple principles, while being governed by additional phenomena such as 1D density of states (DOS), ballistic transport, and phonon scattering.

Planar CNTFETs (Fig. 8a) constitute the majority of devices fabricated to date, mostly due to their relative simplicity and moderate compatibility with existing manufacturing technologies. The coaxial geometry (Fig. 8b) maximizes the capacitive coupling between the gate electrode and the nanotube surface, thereby inducing more channel charge at a given bias than other geometries. This improved coupling is desirable in mitigating the short-channel effects that plague technologies like CMOS as they downside device features. The key device dimensions are: the gate inner radius, R_g, and thickness, t_g; the nanotube radius, R_t, and length L_t; the insulator thickness $t_{ins} = R_g - R_t$; the end-contact radius, t_c (the source and drain may sometimes be of different sizes), and length, L_c; and the gate-underlap L_u.

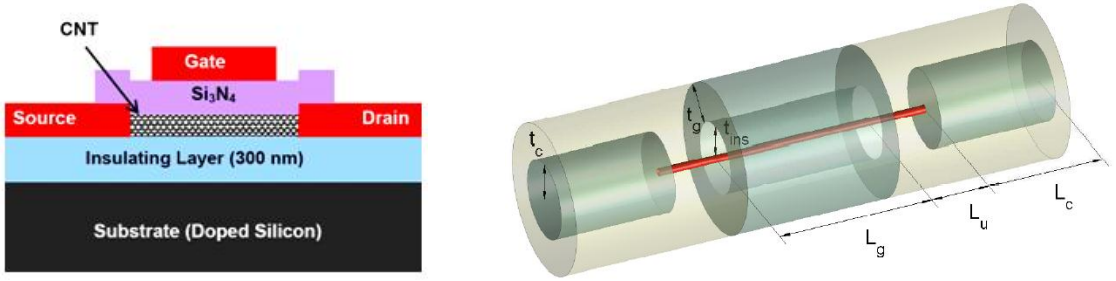

(a) (b)

Fig. 8 Structures of CNTFETs: (a) planar CNTFET, (b) coaxial CNTFET

5) Spin Field Effect Transistor:

In the late 1989 Supriyo Datta and Biswajit Das from Purdue University proposed an electron wave analog of the electro-optic light modulator. Most of the today's interest in spintronics is motivated by their well-known proposed device which is known as the spin field-effect transistor (spin FET).

Datta-Das paper spurs new research direction. Datta-Das spin field effect transistor is a tree-terminals device containing source, drain and gate. The operation of ideal Datta-Das spin FET can be sketched in Fig. 9.

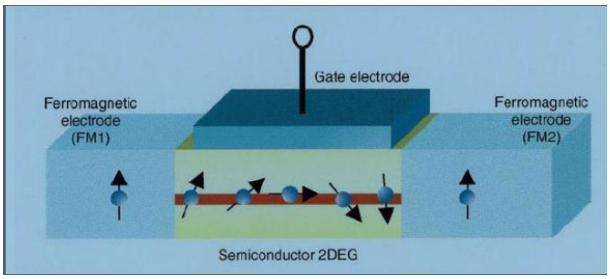

Fig. 9 Basic configuration of a spin field-effect transistor proposed by Datta-Das

Using "menu" of the main screen we can choose materials, temperature, gate thickness, gate length for simulation of I_D-V_D characteristics of spin FET (Fig. 10). Seven semiconductors used for channel such as GaAs, Si, $In_{0.75}Ga_{0.25}As$, $In_{0.75}Al_{0.25}As$, InAs, InSb, $Hg_{0.775}Cd_{0.225}Te$ can be chosen for constructing channel of spin FET by using menu. I_D-V_D curves can be divided into two regions: linear and saturation. Drain current, I_D starts from zero and increases linearly when drain voltage, V_D is small. I_D is not changed when V_D is greater than ($V_G - V_{th}$), where V_{th} is threshold voltage.

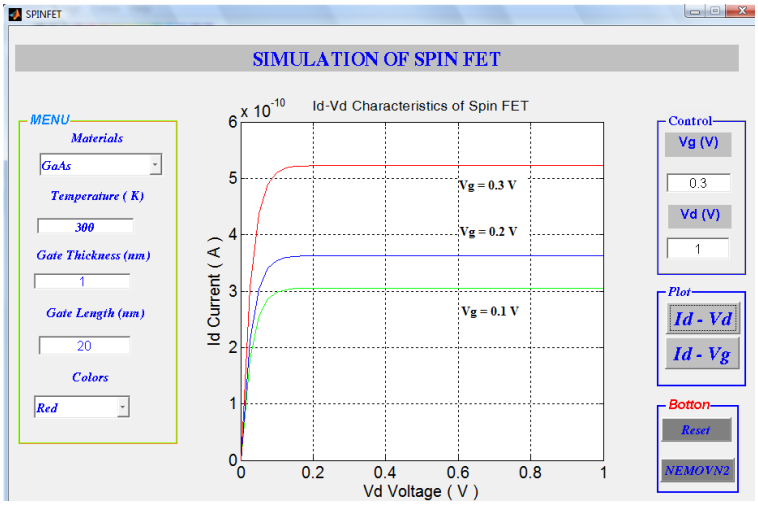

Fig. 10 Typical I_D-V_D characteristics of spin FET simulated by the simulator NEMO-VN2 for various values of V_G = 0.3 V, 0.2 V and 0.1 V at room temperature, T = 300 K. The spin FET parameters are: material, GaAs; L_G = 20 nm; the gate thickness of 1 nm.

Fig. 11 shows the I_D-V_G characteristics of the spin FET having the length of 20 nm at differential drain voltages, V_D = 0.5 V, 0.4 V, 0.3 V, and 0.2 V.

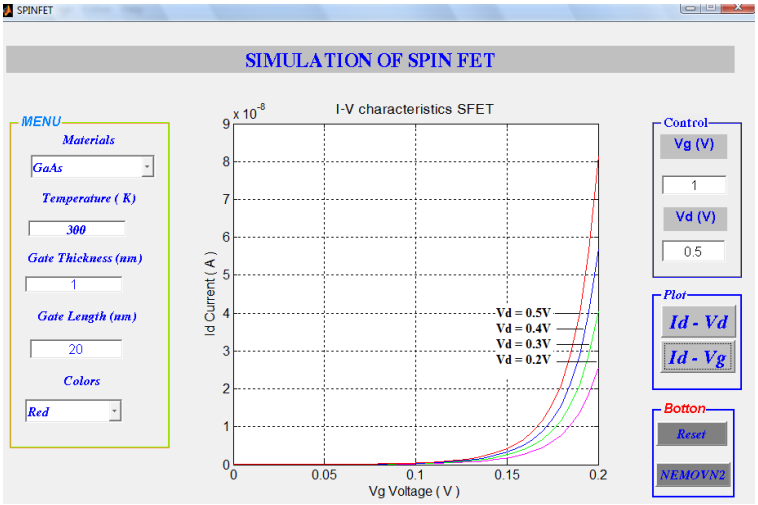

Fig. 11 Typical I_D-V_G characteristics of spin FET simulated by the simulator NEMO-VN2 for various values of V_D = 0.5 V, 0.4, 0.3 and 0.2 V at room temperature, T = 300 K. The spin FET device parameters are: material, GaAs, L_G = 20 nm, the gate thickness is 1 nm.

6) Top-Gate Graphene Field Effect Transistor:

Top-gate graphene field effect transistor is a tree-terminals device consisting of source, drain and gate. Top-gate graphene FET as shown in Fig. 12 is simulated. The normal device has a top gate insulator of Al_2O_3 [31].

We start by simulating I_D-V_D characteristics of top-gate graphene FET. Fig. 12 shows the schematic of the device used in our simulations. Top-gate graphene FET with two-dimensional graphene as the channel is simulated. The device is simulated with Al_2O_3 as the dielectric which has been predicted to be one of the promising dielectrics for graphene FETs in recent experiment [31]. All the simulations have been done for channel length of the graphene FET, L = 20 nm.

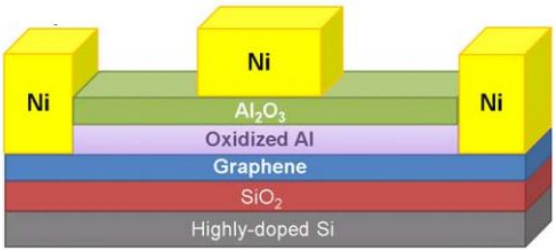

Fig. 12 Structure of top gated graphene field-effect transistor [31]

Fig. 13 shows the I_D-V_D characteristic of the graphene FET having the length of 20 nm at the gate voltage, V_G = 0.5 V. This behavior is in agreement with experimental results [31].

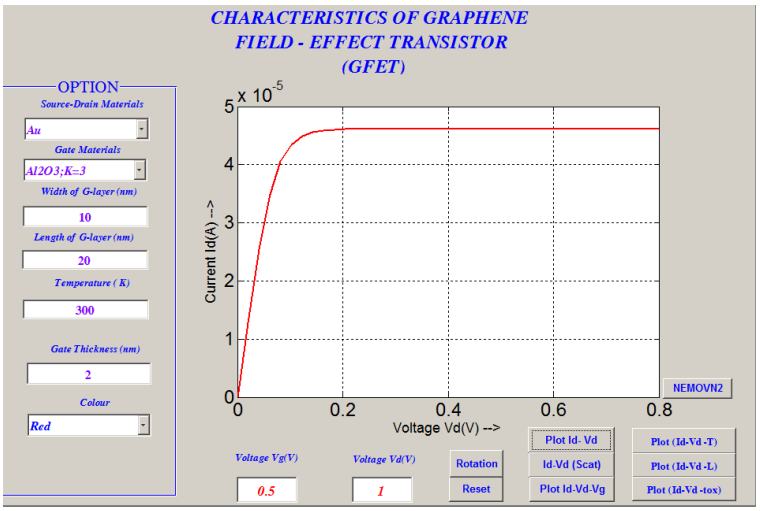

Fig. 13 The I_D-V_D characteristic of the top gate graphene field-effect transistor at the gate voltage, V_G = 0.5 V

The 3D current-voltage characteristics of the top-gate graphene field effect transistor shows in Fig. 14.

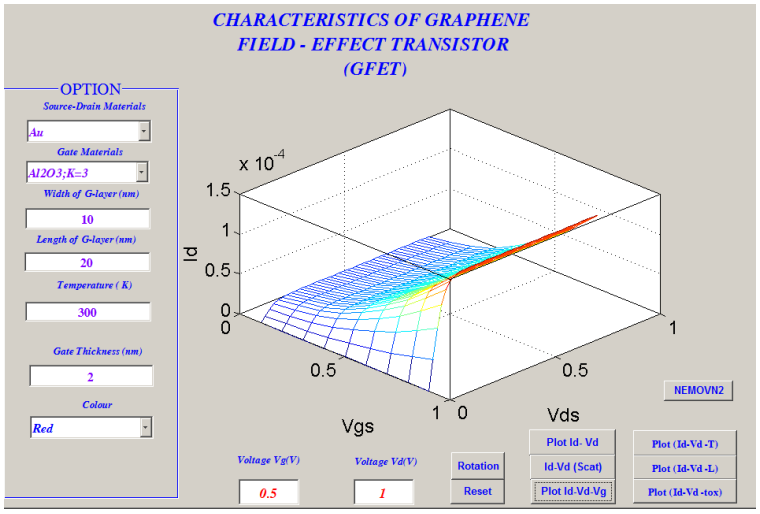

Fig. 14 The 3D I_D-V_D-V_G characteristics of the top-gate graphene field-effect transistor

III. CONCLUSIONS

We present briefly here the description of the upgraded simulator, NEMO-VN2. The NEGF method is used to simulate transport of carriers in all quantum devices such as the resonant tunneling diode, the single electron transistor, the molecular field effect transistor, the planar and coaxial CNTFETs, the spin FET, and the top-gate graphene FET. We also demonstrate

abilities of the NEMO-VN2 for simulating nanodevices using GUI in Matlab. Finally, we present some new simulation results obtained by this simulator, such as the current-voltage characteristics.

ACKNOWLEDGEMENT

This work is funded by VNU-HCM City under research grant C2013-18-14.

REFERENCES

[1] The international Technology Roadmap for Semiconductor, 2005 Edition.

[2] Dinh Sy Hien, Development of quantum device simulator, NEMO-VN2, *Proc. of fifth IEEE International Symposium on Electronics Design, Test and Applictions, DELTA 2010*, 13-15 Jan. 2010, HCM City, p. (170-173), 2010.

[3] Dinh Sy Hien, Modeling of carbon nanotube field effect transistors, *Carbon nanotube applications on electron devices* edited by Jose Mauricio, Marulanda, Intech, p. (187-212), 2011.

[4] Dinh Sy Hien, Development of quantum simulator for emerging nanoelectronics devices, *Journal of ISRN Nanotechnology*, vol.2012, doi: 10.5413/2012/617214, 2012.

[5] M. N. Baibich, J. M. Broto, A. Fert, F. Nguyen Van Dau, F. Petroff, P. Etienne, G Creuzet, A. Friederich, and J. Chazelas, Giant magneto resistance of (001)Fe/(001)Cr magnetic superlattices, *Physical Review Letters* vol. 61, p. (2472-2475), 1988.

[6] G. Binasch, P. Grunberg, F. Saurenbach, and W. Zinn, Enhanced magneto resistance in layered magnetic structures with anti-ferromagnetic interlayer exchange, *Phys. Rev. B*, vol. 39, p. (4828-4830), 1989.

[7] J. Daughton, J. Brown, E. Chen, R. Beech, A. Pohm, and W. Kude, Magnetic field sensors using GMR multilayer, *IEEE Trans. Magn.*, vol. 30, No. 6, p. (4608-4610), 1994.

[8] S. Datta and B. Das, Electronic analog of the electro-optic modulator, *Appl. Phys. Lett.*, vol.56, p. (665-667), 1990.

[9] K.S Novoselov, A.K. Giem, S.V. Morozov, D. Jang, Y. Zhang, S.V. Dubonos, I.V. Grigorieva, and A.A. Firsov, Electric field effect in atomically thin films, *Science*, vol. 306, N0 5696, p. 666-669, 2004.

[10] L. Jiao, L. Zhang, X. Wang, G. Diankov, and H. Dai, Narrow graphene nanoribbons from carbon nanotubes, *Nature*, vol. 458, p. 877-880, 2009.

[11] X. Li, X. Wang, L. Zhang, S. Lee, H. Dai, Chemically drived, ultrasmooth graphene nanoribbon semiconductors, *Science*, vol. 319, No. 5867, p. 1229-1232, 2008.

[12] K.I. Bolotin, K.J. Sikes, Z. Jiang, G. Fundenberg, J. Hone, P. Kim, and H.L. Stormer, Ultrahigh electron mobility in suspended graphene, *Solid State Comm*., vol. 146, p. 351-355, 2008.

[13] M.S. Purewal, Y. Zhang, and P. Kim, Unusual transport properties in carbon based nanoscaled materials: nanotubes and graphene, *Phys. State Sol*.(b), vol. 243, No.13, p. 3418-3422, 2006.

[14] J.S. Moon, D. Curtis, M. Hu, D. Wong, P.M. Campbell, G. Jernigan, J.L. Tedesco B. Vanmil, R. Myers-Ward, C. Eddy, and D.K Gaskill, Epitaxial graphene RF field-effect transistors on Si-face 6H-SiC substrates, *IEEE electron device Lett*., vol. 30, No. 6, p. 650-652, 2009.

[15] Y.M. Lin, C. Dimitrakoponlos, K.A. Jenkins, D.B. Farmer, H.Y. Chiu, A. Grill, Ph. Avouris, 100-GHz transistors from wafer-scale epitaxial graphene, *Science*, vol.327, No. 5966, p. 662, 2010.

[16] Y.Q. Wu, P.D. Ye, M.A. Capano, Y. Xuan, Y. Sui, M. Qi, J.A. Cooper, T. Shen, D. Pandey, G. Prakash, and R. Reifenberger, Top-gate graphene field effect transistors formed by decomposition of SiC, *Appl. Phys. Lett.*, vol. 92, No.9, p. 092102, 2008.

[17] E.H. Hwang and S. Das Sarm, Dielectric function and plasmons in two-dimentional graphene, *Phys. Rev. B*, vol. 75, No. 20, p. 0205418, 2007.

[18] E.H. Hwang and S. Das Sarma, Acoustic phonon scattering limited carrier mobility in two-dimentional extrinsic graphene, *Phys. Rev. B*, vol. 77, No. 11, p. 115449, 2008.

[19] J.H. Chen, C. Jang, S. Xiao, M. Ishigami, and M.S. Fuhrer, Intrinsic and extrinsic performance limits of graphene devices on SiO_2, *Nat. Nanotech*., vol. 3, p. 206-209, 2008.

[20] T. Ando, Screening effect and impurity scattering in monolayer graphene, *J. Phys. Soc. Japan*, p. 074716, 2006.

[21] I Meric, M.Y. Han, A.F. Young, B. Oezyilmaz, P. Kim, and K. Shepard, Current saturation in zero-bandgap top-gated graphene field-effect transistors, *Nat. Nanotech*., vol.3, p. 654-659, 2008.

[22] I. Meric, C. Dean, A.F. Young, J. Hone, P. Kim, and K. Shepard, Graphene field-effect transistors based on boron nitride gate dielectrics, *IEDM Tech. Dig*., p. 556-559, 2010.

[23] M. Freitag, M. Steiner, Y. Martin, V. Perebeinos, Z. Chen, J.C. Tsang, and P. Avouris, Energy disspation in graphene field effect transistors, *Nano Lett*., vol.9, No. 5, p.1883-1888, 2009.

[24] V.E. Dorgan, M.H. Bae, E. Pop, Mobility and saturation velosity in graphene on SiO_2, *Appl. Phys. Lett.*, vol.97, No.8, p.082112, 2010.

[25] V. Perebeinos and P. Avouris, Inelastic scattering and current saturation in graphene, *Phys. Rev. B*, vol.81, p.195442, 2010.

[26] A.M. Dasilva, R. Zou, J.K. Jain, and J. Zhu, Mechanism for current saturation and energy disspation in graphene transistors, *Phys. Rev. Lett*., vol.104, No.24, p.236601, 2010.

[27] X. Li, E.A. Barry, J.M. Zavada, M. Buongiorno Nardelli, and K.W. Kim, Surface polar phonon dominated electron transport in graphene, *Appl. Phys. Lett.*, vol.97, No.23, p.232105, 2010.

[28] J. Chauhan and J. Guo, High-field transport and velosity saturation in graphene, *Appl. Phys. Lett.*, vol.95, p.023120, 2009.

[29] R.S. Shishin and D.K. Ferry, Velosity saturation in intrinsic graphene, *J. Phys. Condens. Matter*, vol.21, p.344201, 2009.

[30] S. Datta, *Quantum Transport: Atom to Transistor*, Cambridge University Press, (2005).

Hien Dinh Sy is an associate professor on physics of HCM university of science. He was born in Thanhhoa province in Vietnam in 1952. He received a BS degree in Nuclear Physics from Hanoi University in 1974. His degree is in nuclear physics from Vietnam national institute of atomic energy (PhD 1992). His research addresses modeling and simulation of nanoelectronics devices. He has published seven books, one book chapter, over forty five journal papers as well as conference proceedings.